Extending the pMSSM Coverage with 3-jets+E_T^{miss} Simplified Models Results

Federico Ambrogi[1]

University of Vienna, Faculty of Physics, Bolzmanngasse 5, A-1090 Wien, Austria
email: federico.ambrogi88@gmail.com

Received: date / Accepted: date

Abstract. The ATLAS collaboration at the Large Hadron Collider (LHC) analysed in arXiv:1508.06608 the constraints provided by the Run 1 searches, performed at 8 TeV centre-of-mass energy, on a 19-parameters realisation of the phenomenological Minimal Supersymmetric Standard Model (pMSSM). It was shown in arXiv:1707.09036 that a large fraction of the parameter space of this model can be efficiently constrained by means of simplified models spectra (SMS) results, and potentially new simplified models result could cover the missed part, by extending the interpretation of the existing searches to new simplified models. This work aims at demonstrating that by recasting existing searches with a simplified model, that originates an experimental signature as simple as 3jets + E_T^{miss} , extends significantly the constraining power of SMS results on the pMSSM-19.

1 Introduction

Simplified models spectra (SMS) have become the standard method for the LHC collaborations to interpret the results of their searches for Beyond the Standard Model (BSM) particles, as in the case of Supersymmetry (SUSY). The most notable benefit coming from the adoption of SMS is the reduction of the large parameter spaces of full theories. With SMS, the impact of the LHC searches can be understood by introducing only a handful of new parameters. Only a few SUSY particle appears in each SMS, while all the remaining are considered decoupled, i.e. their masses are too large so that the production cross section at the LHC is negligible, and they do not appear as intermediate on-shell states in cascade decays.

In the case of SUSY, the masses of the of the particles, their production cross section and their decay modes are sufficient to fully characterise the results of the searches, and once these parameters are fixed, it is straightforward to estimate the exclusion provided by the LHC searches in terms of SMS. The interpretation of SUSY searches with SMS started back at the early LHC era, with the data collected at a centre-of-mass energy of 7 TeV. In [?], the CMS Collaboration summarised the main feature of the most common SMS used for the interpretation of the searches. The choice of such was driven by the sensitivity of the searches to the simple experimental signature provided by those SMS, and in particular it was stressed how the kinematics of the events was determined mainly by the mass scale of the SUSY particles involved, rather than other less important quantum or gauge numbers. While SMS prove useful to reduce the complexity of a full SUSY, or in general BSM theory, they require dedicated efforts to use such results to constrain arbitrary models that share similar kinematics properties. The main limitation concerns possibly complicated particle spectra and thus cascade decays to the lightest supersymmetric particles (LSP), whose kinematics might differ significantly from the simplified case. Moreover, by definition, the number of free parameters, i.e. of free particle masses in SMS should be kept small, and essentially the SMS commonly used for the interpretation of searches go up to three SUSY particles masses for cascade decays, or for asymmetric production (production of two different SUSY particles).

For the task of re-interpretation of searches with SMS results, dedicated tools such as `FastLim` [?] and `SModelS` [?] were developed. They can decompose the signal of SUSY models into its SMS, and check the constraints provided by the LHC searches, contained in a dedicated database of results. In particular, `SModelS`was used in [1] to study the coverage of the pMSSM-19 with SMS with respect to the full recast analyses performed by the ATLAS collaboration. Specifically, the set of pMSSM points considered were made public by the ATLAS collaboration on the `HepData` website [2]. The sensitivity of the ATLAS searches for a selection of BSM searches on the pMSSM was presented in [?]. By re-running their analyses on thousands of pMSSM model points, they could characterise the regions of the parameter space according to the nature of the LSP, represented in this model by the lightest of the four neutralinos, divided into Bino, Higgsino and Wino-like nature, as:

- **Bino-like LSP** when $N_{11}^2 > max(N_{12}^2, N_{13}^2 + N_{14}^2)$ [103,410];
- **Wino-like LSP** when $N_{12}^2 > max(N_{11}^2, N_{13}^2 + N_{14}^2)$ [80,233];
- **Higgsino-like LSP** when $(N_{13}^2+N_{14}^2) > max(N_{11}^2, N_{12}^2)$ [126,684],

where N_{ij} are the entries in the neutralino mixing matrix (see e.g. []), and in square brackets the total numbers of parameters points tested in the ATLAS study.
The same model points were then tested with `SModelS`v1.1 [**?**], obtaining a total coverage of roughly 55%-63% for the Bino and Higgsino-like LSP case, respectively. [1]. The work also showed that by means of efficiency maps (EM) results, that can be produced by phenomenologists outside the experimental collaborations, it was possible to increase significantly the number of excluded point. This is mainly due to the fact that the LHC collaborations provide results only for a limited set of SMS, and many interesting model, to which existing searches are sensitive to, are left unexplored.

Indeed, the comparison between the `SModelS` approach and the re-interpretation performed by the ATLAS collaboration showed that the main limitation of the simplified model approach is the lack of results for simple signatures, such as the $3jets + E_T^{miss}$. One of the `SModelS` tool main features is the ability of extracting the most relevant signatures in terms of $\sigma \times BR$ (production cross section times branching ratio) that are not currently constrained by simplified models results, called *missing topologies*. The aforementioned $3jets + E_T^{miss}$ signature can arise, for example, from gluino-squark associated production, where the gluino decays preferentially to an on-shell lighter squark, in turn decaying to a quark (that is reconstructed by the analysis as a jet of hadrons) and the LSP. This simplified model can be fully described by three mass parameters of the sparticle involved: $m_{\tilde{g}}, m_{\tilde{q}}$ and $m_{\tilde{\chi}_1^0}$. However, under the simplified model assumption, results for such model can be used to constrain the alternative mass hierarchy where the squark is heavier than the gluino, so that in this scenario the squark decays to on-shell gluino. The gluino can then decay radiatively to a gluon and the LSP or via an off-shell squark (i.e. 3-body decay, producing a $4jets + E_T^{miss}$ signature), depending on its mass difference with the lightest squark.

The idea at the basis of this paper is to extend the previous study of the coverage of the pMSSM, and concretely show how the inclusion of newly created EM for the $3jets + E_T^{miss}$ signature increases the coverage of the pMSSM. This can be efficiently done by combining the information obtained with `SModelS` regarding the important missing topologies, and the usage of analyses recasting tools to produce EMs results for arbitrary simplified models, to be implemented in the database of experimental results. For this purpose, this paper is structured as follows. Section 2 summarises the main characteristics of the $3jets + E_T^{miss}$ signature arising from gluino-squark production. In Section 3 the set up of the `SModelS`analysis is described: the details regarding the production of the EMs for the gluino-squark model are discussed, and the set of pMSSM points used for the study are provided. Section 4 summarises the improved constrained obtained with the newly added EMs, in particular discussing the benefit of the signal combination from EM results. Finally an outlook about future extensions of the procedure is given in the conclusive Chapter 5.

THE GLUON JET IS WRONG IN THE PIC

2 The 3 jets + E_T^{miss} Signature

In generic pMSSM-19 points, the squark mass parameters are:

$$m_{\tilde{u}_L} = m_{\tilde{d}_L} = m_{\tilde{c}_L} = m_{\tilde{s}_L}$$

$$m_{\tilde{u}_R} = m_{\tilde{c}_R}$$

$$m_{\tilde{d}_R} = m_{\tilde{s}_R}$$

Since the mass of the gluinos is another free parameter, there are two possible mass hierarchies of interest. When considering for simplicity the lightest of the squark masses with $m_{\tilde{g}} > min(m_{\tilde{q}})$ (and the other third generation squark set to a high scale), gluino will decay almost entirely to an on-shell intermediate squark, followed by the decay of the squark to the LSP:

$$\tilde{g} \to \tilde{q}q, \tilde{q} \to q\tilde{\chi}_1^0 \tag{1}$$

However, for the alternative hierarchy where the squark considered is heavier than the gluino, $min(m_{\tilde{q}}) > m_{\tilde{g}}$ the squarks will decay to an on-shell intermediate gluino. The gluino will then decay either via radiative decay to the LSP as

$$\tilde{q} \to \tilde{g}q, \tilde{g} \to g\chi_1^0 \tag{2}$$

or, for small $\Delta M(min(m_{\tilde{q}}), m_{\tilde{g}})$, via a three-body decay from off-shell squark:

$$\tilde{q} \to \tilde{g}q, \tilde{g} \to q\bar{q}\tilde{\chi}_1^0. \tag{3}$$

The last produces a 4-jets "[[['jet','jet']],[['jet'],['jet']]]" signature, will not be considered in this work. The simplified model of interest of this paper is instead the one described by the experimental signature $3jets + E_T^{miss}$ in the Decays 1 and 2, or, using `SModelS` language, by the *[[['jet']],[['jet'],['jet']]]* constrain. This experimental signature can be obtained by considering two different mass hierarchies, which are depicted by the diagrams a) and b) in Fig. 1. The former, labelled *T3GQ* represents the case

[1] The Wino-like LSP dataset was neglected since most of the model pointed included long-lived charged particles, a signature which could not be handled by the v1.1 used.

where the gluinos are heavier than the squarks considered, while the latter, labelled *T3QG* represents the other case. Depending on the specific pMSSM model point considered, one mass hierarchy or the other can potentially produce this particular signature. According to the simplified models assumption adopted by `SModelS` , however, there is no need to distinguish between the two cases, and it is possible to use efficiencies (and the derived cross section upper limits) obtained with the choice of one of the hierarchies to constrain both scenarios. As stated in the introduction, the *T3GQ* model was found to be the most important missing result for the pMSSM. It is to note, however that, by construction, the *T2* and *T5* models, represented by plots c) and d) of Fig. 1, are automatically important when the *T3GQ* model is. In practice, the *T3GQ* model is an asymmetric model composed by one branch from the *T2* and one branch from the *T5* models. Thanks to the usage of EM results, it is thus possible to combine the signals from the $pp \to \tilde{g}\tilde{g}$, $pp \to \tilde{q}\tilde{q}$ and $pp \to \tilde{g}\tilde{q}$ channels. Along with the results from *TGQ*, the power of combining the *T2* and *T5* models will be explored in this work. For completeness, results for the *T2* and *T5* models were already included in the previous release of the database, hence did not appear in the missing topologies list of the original study.

3 Description of the Analysis Setup

In this Section we describe the setups of the Monte Carlo production followed by the analysis recasting for the extraxtion of the efficiency maps, followed by the description of the analysis of the constraints on the pMSSM with simplified models with the `SModelS` tool.

3.1 Production of the Efficiency Maps

The set-up for the production of the Monte Carlo signals is the following. Events at parton level were generated using `MadGraph5_aMC@NLO` [?], and then showered and hadronized using `Pythia 6.4` [3]. The processes considered for the production of the samples for the simplified model are described in Tab. 1. Note that the processes considered the emission of up to one extra parton. The syntax $\$go\ Q$ is used to avoid the presence of on-shell resonances, represented by intermediate gluino or squarks, that would lead to double counting when performing the merging between matrix-element and parton-shower. The merging between the matrix elements and parton-shower formalisms was performed adopting the k_T *jet* MLM scheme [4,5]. The analysis recasting was performed with `MadAnalysis 5`, using the recasting codes for the analysis ATLAS-SUSY-2013-02 [6,7] and CMS-SUS-13-012 [8,9]. The tuned version of `DELPHES 3` integrated in the `MadAnalysis 5` framework was used to perform the simulate the detector effects on the particle objects. Jets were clustered using `FastJet` [10]. The description of the grid of mass points defined for the production of the efficiency maps is provided in Tab. 2. The analyses chosen for the recasting search for SUSY events in the all hadronic final state, vetoing the presence of isolated leptons. In particular the two above analyses are sensitive to events with small jet multiplicity, as generated by the simplified models considered. Although official EM results for the *T2* model were made public by the collaborations, part of the parameter space with small mass gap between the squark and the LSP is below 50 GeV is not properly covered. For this reason, EMs were produced to replace the official results, up to a mass difference as small as 5 GeV between the squarks and the LSP. In addition, also the results for the *T5* model were extended to cover scenarios with small mass difference between the gluino-squark and squark-neutralino. The parameter x is defined so that $m_{\tilde{q}} = x \cdot m_{\tilde{g}} + (1-x) \cdot m_{\tilde{\chi}_1^0}$. For the *T3GQ* model, the gluino mass reaches the value of 2 TeV, with a binning of 50 GeV for $200 \leq m_{\tilde{g}} < 1200$, and a binning of 100 GeV for $1200 \leq m_{\tilde{g}} \leq 2000$ GeV. The squark masses for the *T3GQ* have a 50 GeV binning, and reach the maximum value of 1 TeV. For a better coverage of the parameter space in the case of small mass differences, additional mass planes parametrized with $\Delta M(\tilde{q}, \tilde{\chi}_1^0)$=(5,10,15) GeV were produced. Note that the values of the maximum values of the gluinos and squarks were chosen arbitrarily, since a priory there is no possibility to determine the efficiency of the analysis and of the cross section upper limit. The mass hierarchy used for the production of

`MadGraph5_aMC@NLO` processes
T2: $pp \to \tilde{q}\tilde{q}$ define Q = dl dr dl~dr~ul ur ul ~ur~ generate p p > Q Q add process p p > Q Q j
T5: $pp \to \tilde{g}\tilde{g}$ generate p p > go go add process p p > go go j
T3GQ: $pp \to \tilde{g}\tilde{q}$ define Q = dl dr dl~dr~ul ur ul~ur~ generate p p > go Q $ go Q add process p p > go Q j $ go Q

Table 1. `MadGraph5_aMC@NLO` processes for the production of the Monte Carlo samples.

Mass Planes	
T2: $pp \to \tilde{q}\tilde{q}$	
-	$\min(\Delta M(\tilde{q}, \tilde{\chi}_1^0)) = 5$ GeV
T5: $pp \to \tilde{g}\tilde{g}$	
x=(0.05,0.50,0.95)	
$\Delta M(\tilde{q}, \tilde{\chi}_1^0) = 5$ GeV	
T3GQ: $pp \to \tilde{g}\tilde{q}$	
$m_{\tilde{g}} = 200,\ldots,1200$	50 GeV bin
$m_{\tilde{g}} = 1300,\ldots,2000$	100 GeV bin ($m_{\tilde{g}} \leq 2$ TeV)
$m_{\tilde{q}}$	50 GeV bins ($m_{\tilde{q}} \leq 1$ TeV)
	$\min(\Delta M(\tilde{q}, \tilde{\chi}_1^0)) = 5$ GeV

Table 2. Mass plane parametrization used for the EMs production of the *T2*, *T3GQ* and *T5*. See the text for details.

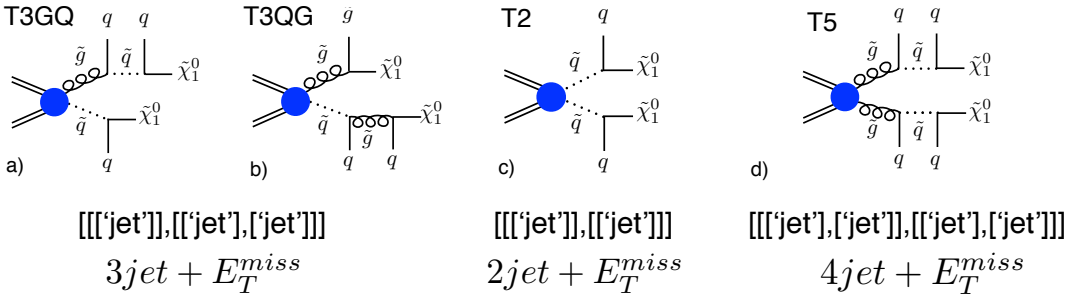

Fig. 1. Diagrams for the simplified models used for the extension of the database. Models *T3GQ*(a) and *T3QG*(b), corresponding to the two different mass hierarchies $m_{\tilde{g}} > m_{\tilde{q}}$ and $m_{\tilde{q}} > m_{\tilde{g}}$, are identified by the experimental signature *[[['jet']],[['jet'],['jet']]]* in `SModelS` notation. Diagrams c) and d) represent the *T2* and *T5* models, mapping to the *[[['jet']],[['jet']]]* and *[[['jet'],['jet']],[['jet'],['jet']]]* signatures.

the gluino-squark model is $m_{\tilde{g}} > m_{\tilde{q}}$, meaning that the *T3GQ* model was chosen to constrain the "[[['jet']],[['jet],['jet']]]" signature. Note that the same problem related to the choice of the mass hierarchy applies to the *T5* model: the "[[['jet']],[['jet']]]" signature can be obtained both with $\tilde{g} \to g\tilde{\chi}_1^0$ and $\tilde{q} \to q\tilde{\chi}_1^0$. Also for the recasting of this model the former hierarchy was chosen. In Appendix **??** the comparison between the values of the upper limits and efficiencies obtained for the two different mass hierarchy, for two benchmark points, are provided. Differences can indeed arise due to the different hadronisation and clustering of quarks and gluon into jets, so that the jets momentum and multiplicity, and linked kinematics variables such as the hadronic transverse energy, might differ. However such differences have a limited impact in the efficiency selection, typically contained within 20%. The observed UL calculation, however, is based on the selection of best expected signal region, i.e. the signal region which provides the best expected limit. The observed number of events indeed suffer from statistical fluctuation, that might be quite different from one signal region to another. For this reason, a small difference in the efficiency might lead to the selection of a different signal regions providing the best expected limit, and consequently to a discording observed UL from SR to SR. While this might result in up to a factor 2 difference in the observed UL, this translates into a modest uncertainty in the cross section UL and in the mass of the related SUSY particle, with little impact in the general interpretation of the excluded regions of the parameter space of the tested pMSSM-19.

3.2 SModelS Analysis

The setup for the analysis with `SModelS` follows closely what described originally in [1], that is here summarized. The pMSSM-19 model points considered represent a subset of the points originally used by the ATLAS collaboration in the re-intepretation study [11], and made available on `HepData` [2]. Only the points that were found to be excluded by at least one of the 8 TeV centre-of-mass energy searches are here considered. Since the main interest is to quantify the coverage of the pMSSM by means of simplified model results, model points that could be excluded only by searches for resonant heavy Higgs bosons, or by searches for exotic charged particle that give origin to signatures such as displaced vertices, were not considered. This selection reduced the original number of points tested by ATLAS from 103,410 to 38,575 (Bino-like LSP dataset) and from 126,684 to 45,594 (Higgsino-like LSP dataset). This identical dataset was used in the previous `SModelS`analysis, and it is now re-analysed, aiming at showing the improvement in the coverage thanks to the newly added efficiency maps results.
Version v1.1.1 of `SModelS` was employed. The `SModelS` cross section calculator, which provides a useful interface with `Pythia 8`(`v.8.226`) [12], `Pythia 6` [3] and `NLLFast` [13–20] was used to compute the production cross sections, up to NLO+NLL order for strong production, and LO for electroweak processes; `Pythia 6` was instead used for slepton production. The other two relevant parameters selected in the configuration file `parameters.ini` are the `sigmacut`= 0.03 fb, that controls the minimum allowed weight $w = \sigma \times BR$ for each simplified model appearing in the decomposition, and `minmassgap` = 5 GeV, i.e. the minimum mass gap for which the SM products appearing in the decay chain are considered visible.

3.3 SModelS Database

We used the complete set of SMS results available for 8 TeV centre-of-mass energy, including official results in the form of upper limits and efficiency maps from the ATLAS and CMS collaborations, EMs results produced by the `FastLim` collaboration available at [**?**] and adapted to the `SModelS` infrastructure, and the set of EM results produced by the `SModelS` collaboration (see the complete description of the database of v1.1 in [1]). We finally added in addition the EM results specifically produced for this work described in Section 3.1.

4 Extending the pMSSM Coverage

In this Section we study the improvements in the pMSSM coverage provided by the additional EMs for the *T3GQ* gluino-squark model, in combination with the *T2* and *T5* model.

Table 3 shows the new total exclusion of the pMSSM points, 21,151 and 28,669 points for the Bino and Higgsino-like case, allowing to cover the 74 and 71 % of the total points tested.

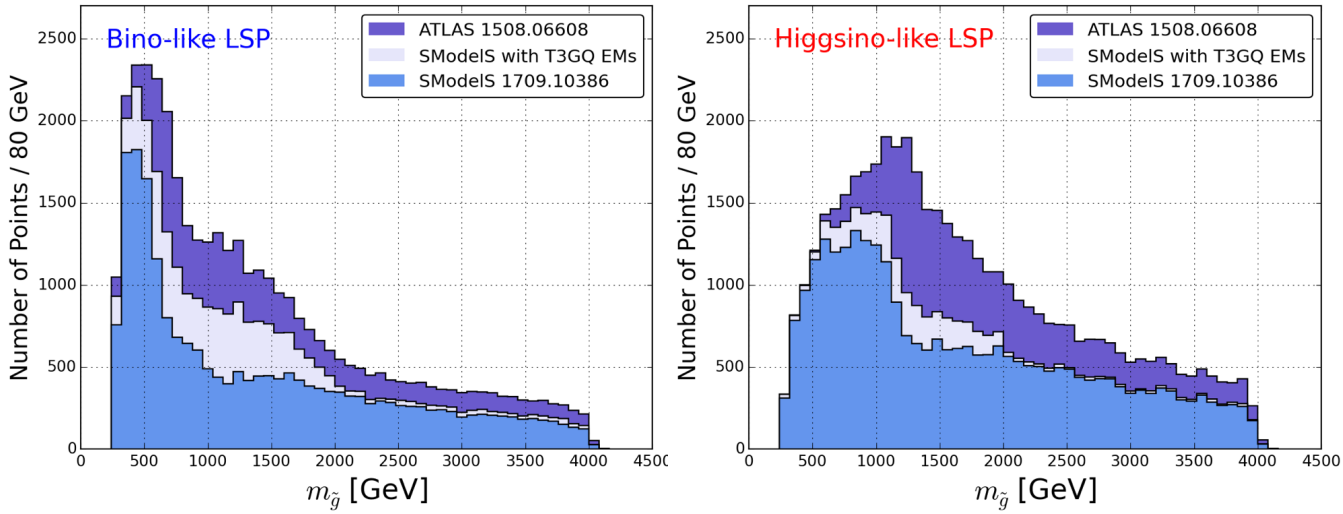

Fig. 2. Distributions of the points excluded by ATLAS (purple), by `SModelS`with the inclusion of the newly homegrown maps (light blue), and by the previous work [1] (slate blue), for the Bino(top) and Higgsino-like LSP (bottom).

With respect to the previous coverage detailed in [1], an improvement in the coverage of +19% and +8% respectively is obtained. The major improvement appears in the Bino-like LSP case, as noticeable also in the gluino and squark mass coverage distributions in Fig. 2. Due to the choice of the parametrisation of the mass planes for the sample production, the bulk of the improvement is found for $m_{\tilde{g}} \leq 2$ TeV. The extension of the EM to cover of the small mass gaps between the squarks and the LSP, as described in Tab. 2, gives important contribution to the exclusion not only for large gluino masses, but also for intermediate to low mass values.

This can be understood by looking at Fig. 3, that reports in colour code the total `SModelS`rvalue for the Bino-like LSP dataset, for the additionally excluded points with respect to the previous study (i.e. excluded by the new EM results). The results are projected in the two mass planes $(m_{\tilde{g}}, min(m_{\tilde{q}})$ and $(m_{\tilde{g}}, m_{\tilde{g}} - m_{\tilde{\chi}_1^0})$. While as a general consideration it can be noticed in both projections that many points exhibit a large rvalue, exceeding the red limit of the colour bar of the plot, this become more evident by looking at the plot that focusses on the small mass gap between the gluinos and the LSP.

	Total	Excluded (EM+UL)
Bino LSP		
	38527	28765 (74 %)
Higgsino LSP		
	45345	32358 (71 %)

Table 3. SModelS constraints for the Bino and Higgsino-like LSP after the addition of the newly implemented EMs results for the models *T2*, *T5* and *T3GQ*.

4.1 Breakdown of the SMS Results

As detailed in Section 2, the *T2*, *T5* and *T3GQ* can be combined to reconstruct more comprehensively the signals from $\tilde{g}\tilde{g}$, $\tilde{q}\tilde{q}$ and $\tilde{g}\tilde{q}$ production channels. Here we wish to analyse how the newly excluded points benefit from such combination. We limit ourselves to consider only the analysis ATLAS-SUSY-2013-02; together with the recast results, EMs for the *T1* model

$$pp \to \tilde{g}\tilde{g}, \tilde{g} \to q\bar{q}\tilde{\chi}_1^0 \tag{4}$$

provided by the ATLAS collaboration are used. The exclusion provided by each model and by the combination of the $T2 + T5 + T3GQ$ are drawn in Fig. **??**. Note that points can be excluded by more than one results, e.g. points with both light squarks and gluinos, with $m_{\tilde{g}} > m_{\tilde{q}}$, might be excluded by both the *T2* and *T5* results; for this reason, the histogram relative to each SMS cannot be stacked together. A major difference between the Bino and the Higgsino-like LSP case concerns the exclusion from the *T1* results, which are significant in the former case, but almost irrelevant in the latter. The model is considered for completeness since such result is available. However, this signal cannot be in general combined with the other signatures of interest, since the *T1* model arises most frequently from the decay of a gluino decaying to an off-shell squark, which is by construction a competing decay channel with respect to the *T3GQ* model. Other SUSY configuration can still result in the *T1* signature, for example the production of charginos and neutralinos decaying hadronically to off-shell vector bosons, but they are practically irrelevant due to the small $\sigma \times BR$.
In Fig. **??** the contribution of the model carrying the largest r value (or partial weight) among the available *T1*, *T2*, *T5* and *T3GQ* is highlighted. For the majority of the points, this values amount to around half of the total weight, calculated using all the available EM results. Besides taking advantage of the availability of recasting tools, EM results are also extremely useful since they allow for the combination of signals, allowing for the reconstruction of full SUSY events. In the case of the *T2*,

T5 and *T3GQ*, the squark-squark, gluino-gluino and gluino-squark productions and their consequent decays to the LSP. Finally, in Fig.??, the distributions of the r values for each result of the analysis ATLAS-SUSY-2013-02 (*T1*, *T2*, *T5* and *T3GQ*), the combinations of models (*T2+T5*, *T2+T5+T3GQ* and the sum of all the available results *T1+T2+T5+T3GQ*) is show. Only the points excluded by the analysis are considered; this implies that the points in the first bin $0 \leq r < 1$ can be excluded only by considering the sum of all the results, i.e. considering *T1+T2+T5+T3GQ*. For the bins with $r \geq 1$, each individual contribution might be sufficient to exclude the models tested. For large rvalues, the number of points decreases as expected, and the importance of the combinations of multiple results increases. The last bin refers to $rvalue \geq 10$, i.e. points that can be strongly excluded by the SMS results considered, in particular by the combination of the *T1+T2+T5+T3GQ* and *T2+T5+T3GQ* for the Bino and Higgsino-like LSP case respectively.

```
ATLAS-02 Bino like excluded ONLY by that txname
Glu_T1_Only 3174
Glu_T2_Only 7221
Glu_T5_Only 191
Glu_TGQ_Only 3259
Glu_T2_T5_TGQ_Only 3320
Total points 24625
***
Glu_T1_Only 204
Glu_T2_Only 11180
Glu_T5_Only 160
Glu_TGQ_Only 2792
Glu_T2_T5_TGQ_Only 299
Total points 22823
```

4.2 Individual SMS r-values

In Figures 5 and ?? the distribution for the r-values for the *T2*, *T5*, *T3GQ* models and their combination is shown, for the Bino and Higgsino-like LSP cases respectively. The contribution from the *T1* model, for which results exist, are not considered. Note that the plots are projected onto the $(m_{\tilde{g}}, min(m_{\tilde{q}}))$ mass plane. This highlights the contribution from the two alternative mass hierarchies $m_{\tilde{g}} > min(m_{\tilde{q}})$ or $min(m_{\tilde{q}}) > m_{\tilde{g}}$, clearly indicated by the points distributed around the diagonal of the plots.

5 Conclusion

Despite a plethora of available simplified model spectra results, in the form of upper limit or efficiency maps, a large portion of the parameter space of a full theory like the pMSSM is left unconstrained. This is a well known fact in the case of model points with complicated mass spectra, that give rise to long decay patterns and for which simplified model are not the adequate method of interpretation of searches. Fortunately there exist a class of simplified models involving only three SUSY particles and short decay chains that captures a large fraction of the signals from gluino-squark associated production. Due to the large production cross section at the LHC, such results prove effective in constraining efficiently the parameter space of the pMSSM-19. It was shown indeed that existing searches for SUSY in the all-hadronic final state are sensitive to the kinematics of such signature, and that thanks to the available recasting tools, it is possible to produce dedicated EM results. The coverage reached thanks to the newly produced results amounts to 74 and 71 % of the official ATLAS exclusion for the Bino and Higgsino-like LSP dataset respectively, and exceed those values for model points with light gluinos.
While recasting tools typically offer more comprehensive constraints, since they can capture all the possible final states arising from the complete decays chains to the LSP, the usage of SMS is more time-efficient. Once the most important missing simplified signatures of a specific model are determined, the production of recast results has to be performed only once, and the results can be re-used by tools such as `SModelS` to constrain generic models. In addition to the possibility to produce customized SMS results, EMs have the advantage of allowing the combination of multiple signals. This is necessary for the exclusion of certain models, for which many production channels are open, or many possible decay chains for the same channel are possible. The importance of the latter was already pointed out in [1] for the decays of third generation squarks via intermediate gauginos, for which the number of available simplified model results is limited, both in diversity and in available mass planes (or mass relations between the three particle masses involved). The analysis of such models, which are important for scenarios compatible with natural SUSY, is of interest. In this work, the combination of the *T2* (squark pair production), *T5* (gluino pair production) and *T3GQ* (gluino-squark production) was investigated, showing that the effective combination os multiple signal can be reconstructed by using the tabulated EM results.

Acknowledgments

The author thanks the Institut für Hochenergiephysik of the Österreichische Akademie der Wissenschaften for the opportunity to use the computing facilities.

References

1. F. Ambrogi, S. Kraml, S. Kulkarni, U. Laa, A. Lessa, and W. Waltenberger, *On the coverage of the pMSSM by simplified model results*, *Eur. Phys. J.* **C78** (2018), no. 3 215, [arXiv:1707.09036].
2. http://hepdata.cedar.ac.uk/view/ins1389857.
3. T. Sjostrand, S. Mrenna, and P. Z. Skands, *PYTHIA 6.4 Physics and Manual*, *JHEP* **0605** (2006) 026, [hep-ph/0603175].
4. S. Hoeche, F. Krauss, N. Lavesson, L. Lonnblad, M. Mangano, A. Schalicke, and S. Schumann, *Matching parton showers and matrix elements*, in *HERA and the LHC: A Workshop on the implications of HERA for LHC physics: Proceedings Part A*, pp. 288–289, 2005. hep-ph/0602031.
5. J. Alwall et al., *Comparative study of various algorithms for the merging of parton showers and matrix elements in hadronic collisions*, *Eur. Phys. J.* **C53** (2008) 473–500, [arXiv:0706.2569].

6. G. Chalons and D. Sengupta, *Madanalysis 5 implementation of the ATLAS multi jet analysis documented in arXiv:1405.7875, JHEP 1409 (2014) 176*, .
7. https://madanalysis.irmp.ucl.ac.be/raw-attachment/wiki/PublicAnalysisDatabase/ma5_atlas_1405_7875.pdf.
8. S. Bein and D. Sengupta, *MadAnalysis 5 implementation of CMS-SUS-13-012*, .
9. http://madanalysis.irmp.ucl.ac.be/raw-attachment/wiki/PublicAnalysisDatabase/ma5_validation_CMS-SUS-13-012.pdf.
10. M. Cacciari, G. P. Salam, and G. Soyez, *FastJet User Manual*, *Eur.Phys.J.* **C72** (2012) 1896, [arXiv:1111.6097].
11. **ATLAS** Collaboration, G. Aad et al., *Summary of the ATLAS experiment's sensitivity to supersymmetry after LHC Run 1 interpreted in the phenomenological MSSM*, *JHEP* **10** (2015) 134, [arXiv:1508.06608].
12. T. Sjostrand, S. Ask, J. R. Christiansen, R. Corke, N. Desai, P. Ilten, S. Mrenna, S. Prestel, C. O. Rasmussen, and P. Z. Skands, *An Introduction to PYTHIA 8.2*, *Comput. Phys. Commun.* **191** (2015) 159–177, [arXiv:1410.3012].
13. http://pauli.uni-muenster.de/~akule_01/nllwiki/index.php/NLL-fast.
14. W. Beenakker, R. Hopker, M. Spira, and P. Zerwas, *Squark and gluino production at hadron colliders*, *Nucl.Phys.* **B492** (1997) 51–103, [hep-ph/9610490].
15. A. Kulesza and L. Motyka, *Threshold resummation for squark-antisquark and gluino-pair production at the LHC*, *Phys.Rev.Lett.* **102** (2009) 111802, [arXiv:0807.2405].
16. A. Kulesza and L. Motyka, *Soft gluon resummation for the production of gluino-gluino and squark-antisquark pairs at the LHC*, *Phys.Rev.* **D80** (2009) 095004, [arXiv:0905.4749].
17. W. Beenakker, S. Brensing, M. Kramer, A. Kulesza, E. Laenen, et al., *Soft-gluon resummation for squark and gluino hadroproduction*, *JHEP* **0912** (2009) 041, [arXiv:0909.4418].
18. W. Beenakker, S. Brensing, M. Kramer, A. Kulesza, E. Laenen, et al., *Squark and Gluino Hadroproduction*, *Int.J.Mod.Phys.* **A26** (2011) 2637–2664, [arXiv:1105.1110].
19. W. Beenakker, M. Kramer, T. Plehn, M. Spira, and P. Zerwas, *Stop production at hadron colliders*, *Nucl.Phys.* **B515** (1998) 3–14, [hep-ph/9710451].
20. W. Beenakker, S. Brensing, M. Kramer, A. Kulesza, E. Laenen, et al., *Supersymmetric top and bottom squark production at hadron colliders*, *JHEP* **1008** (2010) 098, [arXiv:1006.4771].

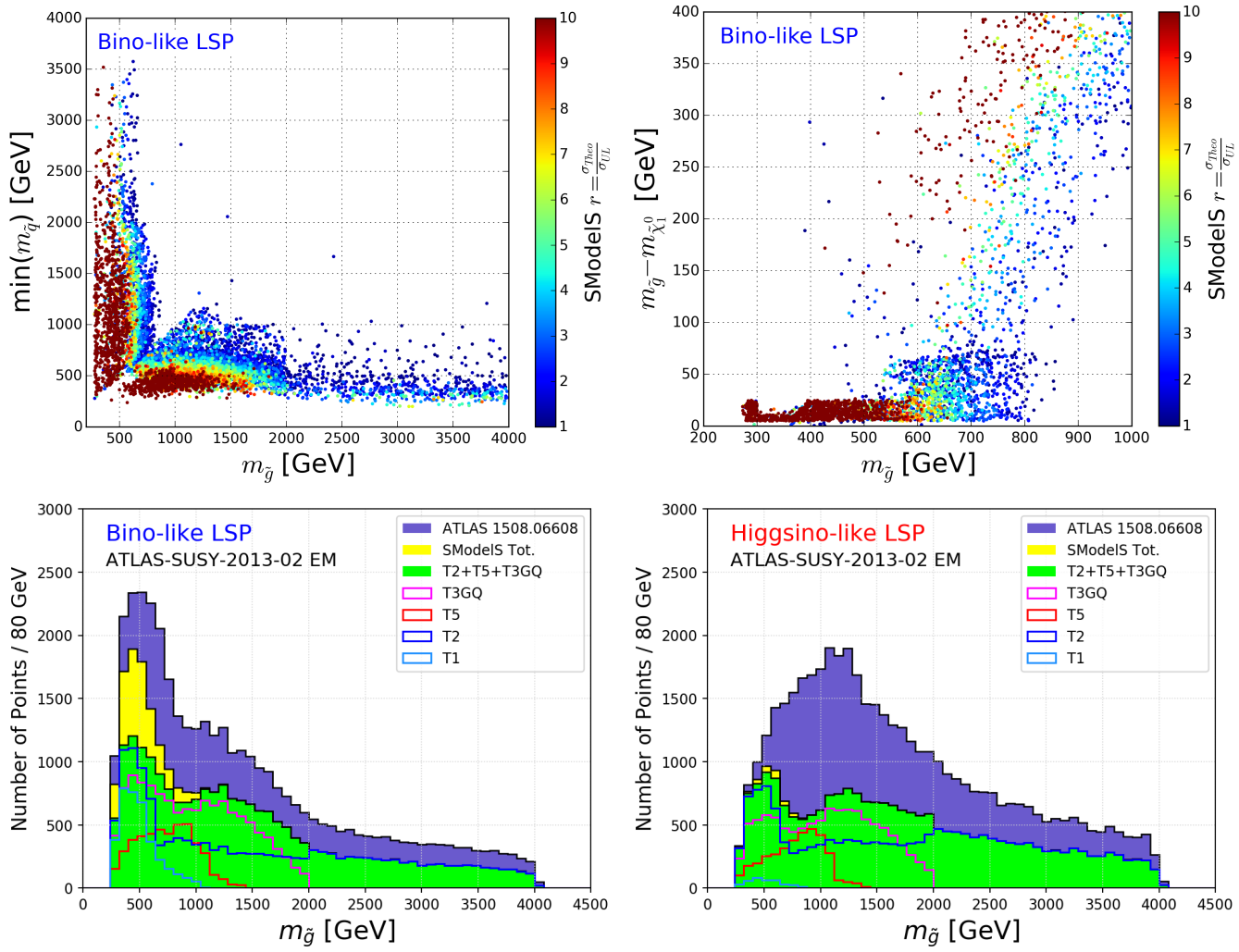

Fig. 3. Top panel: `SModelS` r values for the points excluded by the newly implemented EM results, for the Bino-like LSP in the $(m_{\tilde{g}}, min(m_{\tilde{q}}))$ (left) and $(m_{\tilde{g}}, m_{\tilde{g}} - m_{\tilde{\chi}_1^0})$ mass planes (right). Bottom panel: Contribution of the *T1*, *T2*, *T5* and *T3GQ* simplified model results and their combination for the analysis ATLAS-SUSY-2013-02, as a function of $m_{\tilde{g}}$.

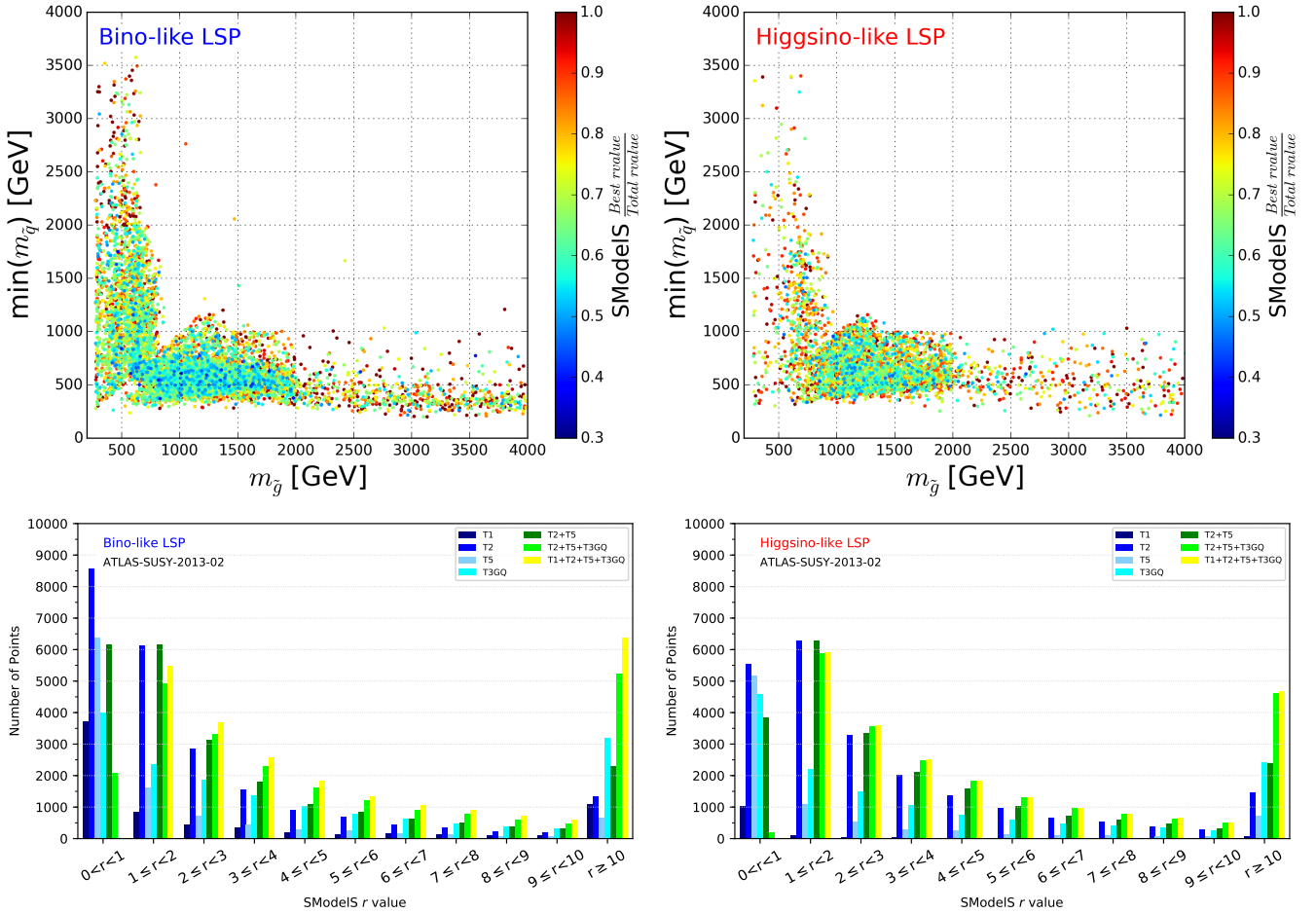

Fig. 4. Top panel: Fractional contribution of the model with the highest r value to the total rvalue. Points in dark blue benefit from the combination of the three results for *T2*, *T5* and XXXXXX. Bottom panel: distribution of the r values for excluded points, considering single SMS or combinations, for the analysis ATLAS-SUSY-2013-02.

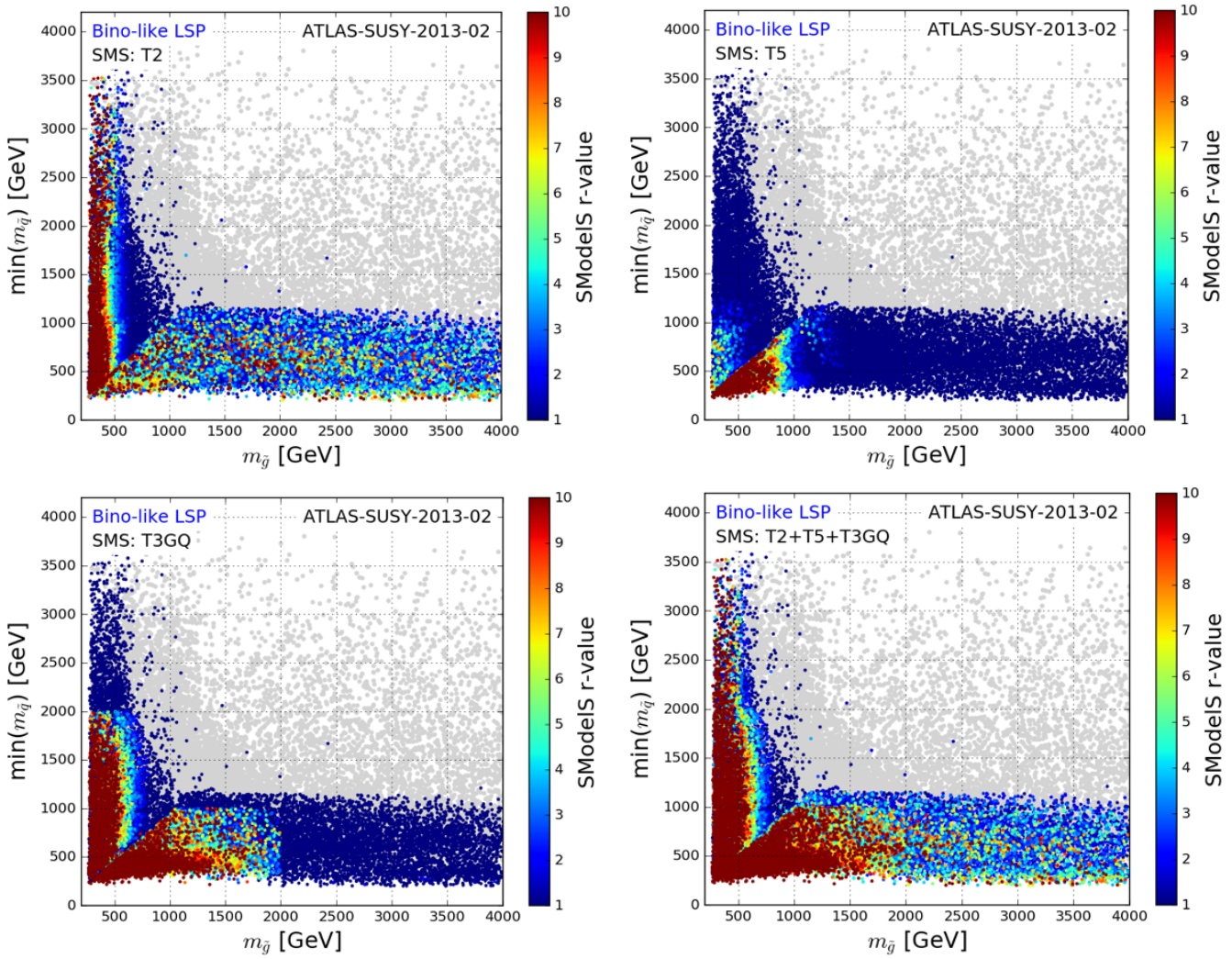

Fig. 5. r value distribution for the *T2*, *T5*, *T3GQ* and their combination for the points excluded using the ATLAS-SUSY-2013-02 analysis alone, for the Bino-like LSP. In grey, the points for which r value ≤ 1 are shown.

A T3GQ vs T3QG Upper Limits

?? The following Tables 4 and 5 compare the upper limits obtained for the mass point $(M_1, M_2, M_3) = (1000, 200, 190), (1200, 600, 500)$ GeV for the two different hierarchy models $T3GQ(m_{\tilde{g}}, m_{\tilde{q}}, m_{\tilde{\chi}_1^0})$ and $T3QG(m_{\tilde{q}}, m_{\tilde{g}}, m_{\tilde{\chi}_1^0})$. In bold, the best SR providing the strongest expected limit and corresponding observed limit is shown. The difference in the efficiency and consequent choice of a different SR, respectively *2jm* for *T3GQ* and *2jt* for *T3QG*, favours a strongest limit for the *T3GQ* case. However the difference is contained within a factor 2, which translates to only few tens of GeV difference in the excluded mass of Squarks or Gluinos. The value of the observed UL, quoted by `SModelS`, is indicated with an asterisk.

$(M_1, M_2, M_3) = (1000, 200, 190)$			**T3GQ**			**T3QG**		
SR	UL_{exp}	UL_{obs}	ϵ	UL_{exp}/ϵ	UL_{obs}/ϵ	ϵ	UL_{exp}/ϵ	UL_{obs}/ϵ
2jm	5.552	4.242	0.118	**47.1**	**36.0**	0.090	**61.5***	**47.0***
2jt	1.512	1.818	0.032	**47.9**	**57.5**	0.027	**56.1**	**67.4**
3j	0.332	0.433	0.002	139.4	182.2	0.002	186.4	243.6
4jl	5.435	4.749	0.032	171.4	149.8	0.039	139.7	122.1
4jl-	11.561	13.292	0.036	318.7	366.4	0.047	248.0	285.2
4jt	0.240	0.149	0.002	146.1	90.8	0.001	178.1	110.8
5j	1.714	1.543	0.007	245.1	220.7	0.010	172.9	155.6
6jl	1.531	1.923	0.002	965.5	1212.5	0.003	555.5	697.7
6jt	0.333	0.332	0.001	472.8	470.4	0.001	327.8	326.2
6jt+	0.302	0.399	0.001	428.6	566.3	0.001	297.2	392.7

Table 4. Summary of the UL for the SRs of ATLAS-SUSY-2013-02, for the *T3GQ* and *T3QG* models, with mass spectrum $(M_1, M_2, M_3) = (1000, 200, 190)$ GeV. In bold, the expected and observed limits for the best SRs are highlited. With a star, the value of the observed UL used by `SModelS`is indicated.

$(M_1, M_2, M_3) = (1200, 600, 500)$			**T3GQ**			**T3QG**		
SR	UL_{exp}	UL_{obs}	ϵ	UL_{exp}/ϵ	UL_{obs}/ϵ	ϵ	UL_{exp}/ϵ	UL_{obs}/ϵ
2jm	5.552	4.242	0.178	31.172	23.815	0.184	30.111	23.004
2jt	1.512	1.818	0.061	**24.623**	**29.601**	0.069	**21.949***	**26.385***
3j	0.332	0.433	0.005	61.421	80.255	0.005	64.971	84.893
4jl	5.435	4.749	0.165	69.892	80.356	0.188	61.542	70.756
4jl-	11.561	13.292	0.145	37.596	32.851	0.166	32.813	28.672
4jt	0.240	0.149	0.004	54.035	33.611	0.004	54.765	34.065
5j	1.714	1.543	0.048	36.043	32.449	0.055	31.004	27.912
6jl	1.531	1.923	0.016	98.361	123.530	0.018	83.039	104.286
6jt	0.333	0.332	0.008	43.713	43.489	0.007	45.136	44.905
6jt+	0.302	0.399	0.008	39.632	52.359	0.007	40.922	54.063

Table 5. Summary of the UL for the SRs of ATLAS-SUSY-2013-02, for the *T3GQ* and *T3QG* models, with mass spectrum $(M_1, M_2, M_3) = (1200, 600, 500)$ GeV. In bold, the expected and observed limits for the best SR are highlited.

B pMSSM19 Parameters

Parameters of the pMSSM-19	
$\tan\beta$	Ratio of the Higgs vacuum expectation values
M_A	Mass of the pseudoscalar Higgs boson
μ	Higgsino parameter
M_1 , M_2 , M_3	Gaugino mass parameters for Binos, Winos and Gluinos
$m_{\tilde{q}}$, $m_{\tilde{u}R}$, $m_{\tilde{d}R}$, $m_{\tilde{l}}$, $m_{\tilde{e}R}$	Masses of 2nd generation sfermions
$m_{\tilde{Q}}$, $m_{\tilde{t}R}$, $m_{\tilde{b}R}$, $m_{\tilde{L}}$, $m_{\tilde{\tau}R}$	Masses of 3rd generation sfermions
A_t , A_b , A_τ	Trilinear couplings for 3rd generation sfermions

Table 6. Description of the free parameters in the pMSSM-19 used by the ATLAS and CMS Collaborations for the re-interpretation study of LHC Run 1 analyses. The label $\tilde{q}$ denotes left-handed squarks, $\tilde{l}$ denotes left-handed sleptons and $\tilde{Q}$ left-handed stops and sbottoms.